

Productions of $D_{s0}^*(2317)$ and $D_{s1}(2460)$ in $B_{(s)}$ and $\Lambda_b(\Xi_b)$ decays

Ming-Zhu Liu^{1,2}, Xi-Zhe Ling³, and Li-Sheng Geng^{4,5,6,7,*}

¹Frontiers Science Center for Rare isotopes, Lanzhou University, Lanzhou 730000, China

²School of Nuclear Science and Technology, Lanzhou University, Lanzhou 730000, China


³Institute of High Energy Physics, Chinese Academy of Sciences, Beijing 100049, China

⁴School of Physics, Beihang University, Beijing 102206, China

⁵Beijing Key Laboratory of Advanced Nuclear Materials and Physics, Beihang University, Beijing 102206, China

⁶Peng Huanwu Collaborative Center for Research and Education, Beihang University, Beijing 100191, China

⁷Southern Center for Nuclear-Science Theory (SCNT), Institute of Modern Physics, Chinese Academy of Sciences, Huizhou 516000, China

 (Received 18 December 2023; accepted 14 February 2024; published 11 March 2024)

Recent studies show that $D_{s0}^*(2317)$ and $D_{s1}(2460)$ contain large molecular components. In this work, we employ the naive factorization approach to calculate the production rates of $D_{s0}^*(2317)$ and $D_{s1}(2460)$ as hadronic molecules in $B_{(s)}$ and $\Lambda_b(\Xi_b)$ decays, where their decay constants are estimated in the effective Lagrangian approach. With the so-obtained decay constants $f_{D_{s0}^*(2317)}$ and $f_{D_{s1}(2460)}$, we calculate the branching fractions of the b -meson decays $B_{(s)} \rightarrow \bar{D}_{(s)}^{(*)} D_{s0}^*$ and $B_{(s)} \rightarrow \bar{D}_{(s)}^{(*)} D_{s1}$ and the b -baryon decays $\Lambda_b(\Xi_b) \rightarrow \Lambda_c(\Xi_c) D_{s0}^*$ and $\Lambda_b(\Xi_b) \rightarrow \Lambda_c(\Xi_c) D_{s1}$. Our results show that the production rates of $D_{s0}^*(2317)$ and $D_{s1}(2460)$ in the B_s , Λ_b , and Ξ_b decays are large enough that future experiments could observe them. In particular, we demonstrate that one can extract the decay constants of hadronic molecules via the triangle mechanism because of the equivalence of the triangle mechanism to the tree diagram established in calculating the decays $B \rightarrow \bar{D}^{(*)} D_{s0}^*(2317)$ and $B \rightarrow \bar{D}^{(*)} D_{s1}(2460)$.

DOI: 10.1103/PhysRevD.109.056014

I. INTRODUCTION

In 2003, the BABAR Collaboration discovered $D_{s0}^*(2317)$ in the $D_s^+ \pi^0$ mass distribution in the $e^+ e^-$ annihilation process [1], which was later confirmed by the CLEO Collaboration [2] and Belle Collaboration [3] in the same process. Moreover, the BESIII Collaboration observed $D_{s0}^*(2317)$ in the process $e^+ e^- \rightarrow D_s^{*+} D_{s0}^{*-}$ [4]. In addition to the above inclusive processes, $D_{s0}^*(2317)$ was also observed in the exclusive process of B decays by the Belle Collaboration [5] and BABAR Collaboration [6]. $D_{s1}(2460)$ as the heavy quark spin symmetry (HQSS) partner of $D_{s0}^*(2317)$ was first discovered in the $D_s^{*+} \pi^0$ mass distribution by the CLEO Collaboration [2] and then confirmed by several other experiments [3,5,7]. Treating $D_{s0}^*(2317)$ and $D_{s1}(2460)$ as conventional P -wave $c\bar{s}$

mesons, the masses obtained in the Godfrey-Isgur model are larger than the experimental ones by 140 and 100 MeV [8], which have motivated extensive discussions on their nature.

By analyzing their masses, several interpretations were proposed for the internal structure of $D_{s0}^*(2317)$ and $D_{s1}(2460)$. In Ref. [9], the authors found that the masses of $D_{s0}^*(2317)$ and $D_{s1}(2460)$ still deviate from the experimental data, even adding the screen potential to the conventional quark model. However, as the DK and D^*K components were embodied in the conventional quark model, the mass puzzles of $D_{s0}^*(2317)$ and $D_{s1}(2460)$ were resolved [10–12], which indicates that the $D^{(*)}K$ components play an important role in forming $D_{s0}^*(2317)$ and $D_{s1}(2460)$. Therefore, $D_{s0}^*(2317)$ and $D_{s1}(2460)$ are proposed to be hadronic molecules of DK and D^*K to explain their masses, especially their mass splitting [13–19]. It should be noted that in the lattice QCD simulation of the DK interaction, a bound state below the DK mass threshold was identified [20–24]. Furthermore, with the $D^{(*)}K$ potentials supplemented by the $c\bar{s}$ core couplings to the $D^{(*)}K$ components, $D_{s0}^*(2317)$ and $D_{s1}(2460)$ can be dynamically generated [25–28], indicating that the $D^{(*)}K$

*lisheng.geng@buaa.edu.cn

Published by the American Physical Society under the terms of the Creative Commons Attribution 4.0 International license. Further distribution of this work must maintain attribution to the author(s) and the published article's title, journal citation, and DOI. Funded by SCOAP³.

molecular components account for a large proportion of their wave functions in terms of the Weinberg compositeness rule $1 - Z$ [25]. Studying the masses of $D_{s0}^*(2317)$ and $D_{s1}(2460)$, one can conclude that they contain both $D^{(*)}K$ molecular components and the $c\bar{s}$ cores. The next natural step forward is to study their decays.

According to the Review of Particle Physics (RPP) [29], the $D_{s0}^{*+}(2317)$ dominantly decays to $D_s^+\pi^0$, which means that $D_{s0}^{*+}(2317)$ must be narrow since the decay of $D_{s0}^{*+}(2317) \rightarrow D_s^+\pi^0$ breaks isospin. The dominant decays of $D_{s1}^+(2460)$ into $D_s^{*+}\pi^0$ and $D_s^+\gamma$ are responsible for its narrow width. The narrow widths of $D_{s0}^*(2317)$ and $D_{s1}(2460)$ are quite different from the widths of their SU(3)-flavor partners $D_0^*(2300)$ and $D_1(2430)$, which reflect the exotic properties of these excited charmed mesons. In Refs. [9,30–33], the authors proposed that the decays of $D_{s0}^*(2317)$ and $D_{s1}(2460)$ as the $c\bar{s}$ excited states into $D_s\pi$ and $D_s^*\pi$ proceed via $\pi - \eta$ mixing, resulting in widths of tens of keV. Treating $D_{s0}^*(2317)$ and $D_{s1}(2460)$ as hadronic molecules, their widths are of the order of 100 keV [34–36]. There are currently no precise experimental measurements of the widths of $D_{s0}^*(2317)$ and $D_{s1}(2460)$, only their upper limits of 3.8 MeV. From the perspective of their widths, one can obtain the same conclusion as from the studies of their masses regarding the nature of $D_{s0}^*(2317)$ and $D_{s1}(2460)$. It is worth noting that a model-independent method has been proposed to verify the molecular nature of $D_{s0}^*(2317)$ by experimental searches for its three-body counterparts DDK and $D\bar{D}K$ [19,37–39].

The discoveries of $D_{s0}^*(2317)$ and $D_{s1}(2460)$ in the inclusive and exclusive processes in e^+e^- collisions triggered a series of theoretical works to investigate their production mechanism. Assuming $D_{s0}^*(2317)$ and $D_{s1}(2460)$ as $D^{(*)}K$ hadronic molecules and $c\bar{s}$ excited states, Wu *et al.* estimated that their production rates in e^+e^- collisions are of the order of 10^{-3} [39], consistent with the experimental data [40]. As for the exclusive process, Faessler *et al.* calculated the decays $B \rightarrow D_{s0}^*(2317)\bar{D}^{(*)}$ and $B \rightarrow D_{s1}(2460)\bar{D}^{(*)}$ assuming $D_{s0}^*(2317)$ and $D_{s1}(2460)$ as $D^{(*)}K$ molecules [41]. The results are a bit smaller than the experimental data. Assuming $D_{s0}^*(2317)$ and $D_{s1}(2460)$ as $c\bar{s}$ excited states, the decays $B \rightarrow D_{s0}^*(2317)\bar{D}^{(*)}$ and $B \rightarrow D_{s1}(2460)\bar{D}^{(*)}$ were investigated as well, but the results suffer from large uncertainties [42–47]. Moreover, the productions of $D_{s0}^*(2317)$ and $D_{s1}(2460)$ in the Λ_b decays have been explored [48] and their production rates in the Λ_b decays were found to be larger than those in the corresponding B decays. Recently, the DK femtoscopic correlation function was investigated to elucidate the nature of $D_{s0}^*(2317)$ [49,50], which could be accessed in high-energy nucleon-nucleon collisions in the future [51,52].

Until now, $D_{s0}^*(2317)$ and $D_{s1}(2460)$ have only been observed in the exclusive process via B decays. In this

work, we systematically explore the productions of $D_{s0}^*(2317)$ and $D_{s1}(2460)$ in $B_{(s)}$ and $\Lambda_b(\Xi_b)$ decays with the factorization ansatz [53,54]. Following Ref. [41], we employ the effective Lagrangian approach to estimate the decay constants of $D_{s0}^*(2317)$ and $D_{s1}(2460)$, which are dynamically generated via the $DK - D_s\eta$ and $D^*K - D_s^*\eta$ coupled-channel potentials described by the contact-range effective field theory (EFT), and then calculate the production rates of $D_{s0}^*(2317)$ and $D_{s1}(2460)$ in $B_{(s)}$ and $\Lambda_b(\Xi_b)$ decays. Another motivation of this work is to test the universality of the approach that we proposed to calculate the decay constant of a hadronic molecule via the triangle mechanism [55]. Based on our previous study of the decays $B \rightarrow D_{s0}^*(2317)\bar{D}^{(*)}$ and $B \rightarrow D_{s1}(2460)\bar{D}^{(*)}$ via the triangle mechanism, the decay constants of $D_{s0}^*(2317)$ and $D_{s1}(2460)$ can be extracted [56]. The effective Lagrangian approach in this work can further check the validity of our approach [55].

This paper is organized as follows. In Sec. II we introduce the effective Lagrangian approach to calculate the productions of $D_{s0}^*(2317)$ and $D_{s1}(2460)$ in $B_{(s)}$ and $\Lambda_b(\Xi_b)$ decays and the decay constants of $f_{D_{s0}^*}$ and $f_{D_{s1}}$. Results and discussions are given in Sec. III, followed by a summary in Sec. IV.

II. THEORETICAL FORMALISM

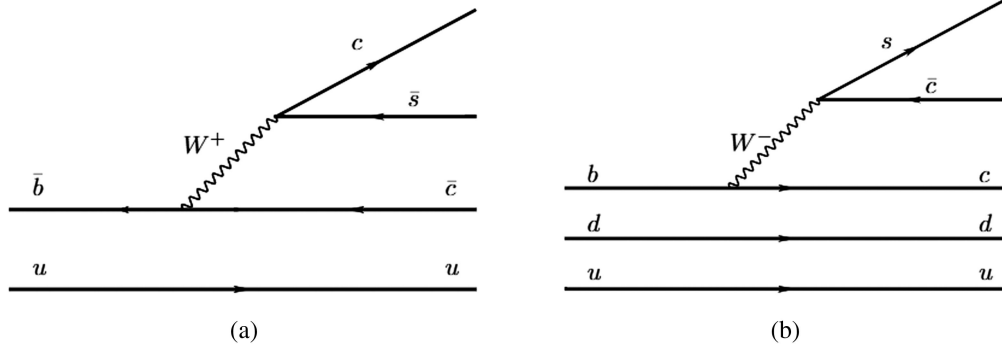
A. Effective Lagrangians for nonleptonic weak decays

In this work, we focus on the productions of $D_{s0}^*(2317)$ and $D_{s1}(2460)$ in $B_{(s)}$ and $\Lambda_b(\Xi_b)$ decays. At quark level, the Cabibbo-favored decays $B^+ \rightarrow \bar{D}^{(*)0}D_s^{*+}$ and $\Lambda_b \rightarrow \Lambda_c D_s^{(*)-}$ mainly proceed via the external W -emission mechanism shown in Fig. 1 according to the topological classification of weak decays [54,57–59], which the naive factorization approach can well describe. With the factorization ansatz [60], the amplitudes of the weak decays $B^+ \rightarrow \bar{D}^{(*)0}D_s^{*+}$ and $\Lambda_b \rightarrow \Lambda_c D_s^{(*)-}$ can be expressed as products of two current matrix elements,

$$\begin{aligned} \mathcal{A}(B^+ \rightarrow D_s^{*+}\bar{D}^{(*)0}) &= \frac{G_F}{\sqrt{2}} V_{cb} V_{cs} a_1 \langle D_s^{*+} | (s\bar{c}) | 0 \rangle \langle \bar{D}^{(*)0} | (c\bar{b}) | B^+ \rangle, \quad (1) \end{aligned}$$

$$\begin{aligned} \mathcal{A}(\Lambda_b \rightarrow D_s^{(*)-}\Lambda_c) &= \frac{G_F}{\sqrt{2}} V_{cb} V_{cs} a_1 \langle D_s^{(*)-} | (\bar{s}c) | 0 \rangle \langle \Lambda_c | (\bar{c}b) | \Lambda_b \rangle, \quad (2) \end{aligned}$$

where G_F is the Fermi constant, V_{cb} and V_{cs} are the Cabibbo-Kobayashi-Maskawa matrix elements, and a_1 is the effective Wilson coefficient. In principle, a_1 is expressed by the Wilson coefficients of the QCD-corrected effective weak Hamiltonian, which depends on the renormalization scale [54,61,62]. In this work, we parametrize the


 FIG. 1. External W -emission mechanism for (a) $B^+ \rightarrow \bar{D}^{(*)0} D_s^{(*)+}$ and (b) $\Lambda_b \rightarrow \Lambda_c D_s^{(*)-}$.

nonfactorization contributions with the effective Wilson coefficient a_1 , which can be determined by reproducing relevant experimental data.

The current matrix elements of $\langle \bar{D}^0 | (c\bar{b}) | B^+ \rangle$ and $\langle \bar{D}^{*0} | (c\bar{b}) | B^+ \rangle$ describing the hadronic transitions are parametrized by six form factors [46],

$$\begin{aligned} \langle \bar{D}^{*0} | (c\bar{b}) | B^+ \rangle = \epsilon_\alpha^* \left\{ -g^{\mu\alpha} (m_{\bar{D}^{*0}} + m_{B^+}) A_1(q^2) + P^\mu P^\alpha \frac{A_2(q^2)}{m_{\bar{D}^{*0}} + m_{B^+}} + i\epsilon^{\mu\alpha\beta\gamma} P_\beta q_\gamma \frac{V(q^2)}{m_{\bar{D}^{*0}} + m_{B^+}} \right. \\ \left. + q^\mu P^\alpha \left[\frac{m_{\bar{D}^{*0}} + m_{B^+}}{q^2} A_1(q^2) - \frac{m_{B^+} - m_{\bar{D}^{*0}}}{q^2} A_2(q^2) - \frac{2m_{\bar{D}^{*0}}}{q^2} A_0(q^2) \right] \right\}, \end{aligned} \quad (3)$$

$$\langle \bar{D}^0 | (c\bar{b}) | B^+ \rangle = \left[P^\mu - \frac{m_{B^+}^2 - m_{\bar{D}^0}^2}{q^2} q_\mu \right] F_1(q^2) + \frac{m_{B^+}^2 - m_{\bar{D}^0}^2}{q^2} q_\mu F_0(q^2), \quad (4)$$

where the momenta $q = p_{B^+} - p_{\bar{D}^{(*)0}}$ and $P = p_{B^+} + p_{\bar{D}^{(*)0}}$, and $F_1(q^2)$, $F_2(q^2)$, $A_0(q^2)$, $A_1(q^2)$, $A_2(q^2)$, and $V(q^2)$ are form factors. The current matrix element $\langle \Lambda_c(p') | \bar{c}b | \Lambda_b(p) \rangle$ is given by [63]

$$\begin{aligned} \langle \Lambda_c(p') | \bar{c}b | \Lambda_b(p) \rangle \\ = \bar{u}(p') \left[f_1^V(q^2) \gamma_\mu - f_2^V(q^2) \frac{i\sigma_{\mu\nu} q^\nu}{m} + f_3^V(q^2) \frac{q^\mu}{m} \right. \\ \left. - \left(f_1^A(q^2) \gamma_\mu - f_2^A(q^2) \frac{i\sigma_{\mu\nu} q^\nu}{m} + f_3^A(q^2) \frac{q^\mu}{m} \right) \gamma^5 \right] u(p), \end{aligned} \quad (5)$$

where $\sigma^{\mu\nu} = \frac{i}{2}(\gamma^\mu \gamma^\nu - \gamma^\nu \gamma^\mu)$ and $q = p - p'$, and $f_i^{V/A}(q^2)$ are form factors. In general, the form factors are parametrized in the following form:

$$\frac{F_i(0)}{1 - a \frac{q^2}{m^2} + b \left(\frac{q^2}{m^2} \right)^2}, \quad (6)$$

where $F_i(0)$, a , and b are parameters determined in phenomenological models. In this work, we take the values of $F_i(0)$, a , and b determined by the quark model [64–66].

The current matrix element $\langle D_s^+ | (s\bar{c}) | 0 \rangle$ describes the process of creating a D_s^+ meson from the vacuum via the axial current, which is parametrized by the decay constant $f_{D_s^+}$ and the momentum of the D_s^+ meson. Following Ref. [44], the current matrix elements for the D_s , D_s^* , $D_{s0}^*(2317)$, and $D_{s1}(2460)$ mesons created from the vacuum are

$$\begin{aligned} \langle D_s^+ | (s\bar{c}) | 0 \rangle = if_{D_s^+} p_{D_s^+}^\mu, \quad \langle D_s^{*+} | (s\bar{c}) | 0 \rangle = m_{D_s^{*+}} f_{D_s^{*+}} \epsilon_\mu^*, \\ \langle D_{s0}^{*+} | (s\bar{c}) | 0 \rangle = f_{D_{s0}^{*+}} p_{D_{s0}^{*+}}^\mu, \quad \langle D_{s1}^+ | (s\bar{c}) | 0 \rangle = m_{D_{s1}^+} f_{D_{s1}^+} \epsilon_\mu^*. \end{aligned} \quad (7)$$

The decay constants of D_s and D_s^* as $c\bar{s}$ ground states are determined to be $f_{D_s} = 250$ MeV and $f_{D_s^*} = 272$ MeV [64]. Due to the exotic properties of $D_{s0}^*(2317)$ and $D_{s1}(2460)$, the estimations of the decay constants $f_{D_{s0}^*}$ and $f_{D_{s1}}$ are quite uncertain. In this work, we estimate the values of $f_{D_{s0}^*}$ and $f_{D_{s1}}$ in the molecular picture. In addition, assuming SU(3)-flavor symmetry, the $B \rightarrow \bar{D}^{(*)}$ and $\Lambda_b \rightarrow \Lambda_c$ transitions can be related with the $B_s \rightarrow \bar{D}_s^{(*)}$ and $\Xi_b \rightarrow \Xi_c$ transitions, and the production mechanisms of $D_{s0}^*(2317)$ and $D_{s1}(2460)$ in the B_s and Ξ_b decays are similar to those

in the B and Λ_b decays, as illustrated in Fig. 1. In the following, we only present the amplitudes for the decays $B \rightarrow \bar{D}^{(*)} D_s^{(*)}$ and $\Lambda_b \rightarrow \Lambda_c \bar{D}_s^{(*)}$, and the amplitudes for the other decays have similar expressions.

With the above effective Lagrangian, we obtain the amplitudes for the decays $B(k_0) \rightarrow \bar{D}^{(*)}(q_1) D_s^{(*)}(q_2)$:

$$\begin{aligned}
\mathcal{A}(B \rightarrow D_s \bar{D}^*) &= \frac{G_F}{\sqrt{2}} V_{cb} V_{cs} a_1 f_{D_s} \left\{ -q_1 \cdot \varepsilon(q_2) (m_{\bar{D}^*} + m_B) A_1(q_1^2) + (k_0 + q_2) \cdot \varepsilon(q_2) q_1 \cdot (k_0 + q_2) \frac{A_2(q_1^2)}{m_{\bar{D}^*} + m_B} \right. \\
&\quad \left. + (k_0 + q_2) \cdot \varepsilon(q_2) [(m_{\bar{D}^*} + m_B) A_1(q_1^2) - (m_B - m_{\bar{D}^*}) A_2(q_1^2) - 2m_{\bar{D}^*} A_0(q_1^2)] \right\}, \\
\mathcal{A}(B \rightarrow D_s \bar{D}) &= \frac{G_F}{\sqrt{2}} V_{cb} V_{cs} a_1' f_{D_s} (m_B^2 - m_{\bar{D}}^2) F_0(q_1^2), \\
\mathcal{A}(B \rightarrow D_s^* \bar{D}) &= \frac{G_F}{\sqrt{2}} V_{cb} V_{cs} a_1^* m_{D_s^*} f_{D_s^*} (k_0 + q_2) \cdot \varepsilon(q_1) F_1(q_1^2), \\
\mathcal{A}(B \rightarrow D_s^* \bar{D}^*) &= \frac{G_F}{\sqrt{2}} V_{cb} V_{cs} a_1^* m_{D_s^*} f_{D_s^*} \varepsilon_\mu(q_1) \left[(-g^{\mu\alpha} (m_{\bar{D}^*} + m_B) A_1(q_1^2) \right. \\
&\quad \left. + (k_0 + q_2)^\mu (k_0 + q_2)^\alpha \frac{A_2(q_1^2)}{m_{\bar{D}^*} + m_B} + i \varepsilon^{\mu\alpha\beta\gamma} (k_0 + q_2)_\beta q_{1\gamma} \frac{V(q_1^2)}{m_{\bar{D}^*} + m_B} \right] \varepsilon_\alpha(q_2). \tag{8}
\end{aligned}$$

In terms of the effective Lagrangian of the weak decays $\Lambda_b(p) \rightarrow \Lambda_c(p') \bar{D}_s^{(*)}(q)$ [67], the corresponding amplitudes are written as

$$\begin{aligned}
\mathcal{A}(\Lambda_b \rightarrow \Lambda_c \bar{D}_s) &= \bar{u}(p') (A + B \gamma_5) u(p), \\
\mathcal{A}(\Lambda_b \rightarrow \Lambda_c \bar{D}_s^*) &= -i \bar{u}(p') \left(A_1 \gamma_\mu \gamma_5 + A_2 \frac{p_{2\mu}}{m} \gamma_5 + B_1 \gamma_\mu + B_2 \frac{p_{2\mu}}{m} \right) u(p) \varepsilon^\mu(q), \tag{9}
\end{aligned}$$

where A_1, A_2, B_1, B_2, A , and B represent the transition form factors of Λ_b to Λ_c :

$$\begin{aligned}
A &= \lambda f_{D_s} \left[(m - m_2) f_1^V + \frac{m_1^2}{m} f_3^V \right], \\
B &= \lambda f_{D_s} \left[(m + m_2) f_1^A - \frac{m_1^2}{m} f_3^A \right], \\
A_1 &= -\lambda f_{D_s^*} m_1 \left[f_1^A - f_2^A \frac{m - m_2}{m} \right], \\
B_1 &= \lambda f_{D_s^*} m_1 \left[f_1^V + f_2^V \frac{m + m_2}{m} \right], \\
A_2 &= 2\lambda f_{D_s^*} m_1 f_2^A, \quad B_2 = -2\lambda f_{D_s^*} m_1 f_2^V, \tag{10}
\end{aligned}$$

with $\lambda = \frac{G_F}{\sqrt{2}} V_{cb} V_{cs} a_1$ and m, m_1, m_2 referring to the masses of $\Lambda_b, \bar{D}_s^{(*)}$, and Λ_c .

With the amplitudes for the weak decays given above, one can compute the corresponding partial decay widths

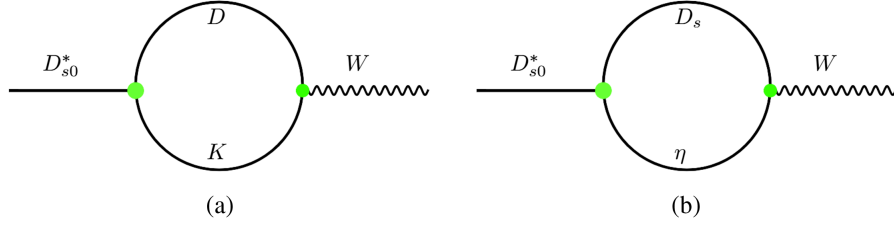
$$\Gamma = \frac{1}{2J+1} \frac{1}{8\pi M^2} |\vec{p}| |\bar{\mathcal{A}}|^2, \tag{11}$$

where J and M are the total angular momentum and the mass of the initial state, $|\vec{p}|$ is the momentum of either final state in the rest frame of the initial state, \mathcal{A} is the amplitude of the weak decay, and the overline indicates the sum over the polarizations of final states.

B. Decay constants

The decay constants $f_{D_{s0}^*}$ and $f_{D_{s1}}$ are defined in Eq. (7). To obtain the values of $f_{D_{s0}^*}$ and $f_{D_{s1}}$, one usually constructs the amplitudes for D_{s0}^* and D_{s1} created from the vacuum and then extracts the coefficients of $p_{D_{s0}^*}^\mu$ and $m_{D_{s1}^*} \epsilon_\mu^*$ [42,44,45,68]. Following the same principle, we calculate the $f_{D_{s0}^*}$ and $f_{D_{s1}}$ decay constants in the molecular picture. Assuming that D_{s0}^* is dynamically generated by the DK and $D_s \eta$ coupled-channel interactions, the current matrix element $\langle D_{s0}^{*+} | (s\bar{c}) | 0 \rangle$ is illustrated in Fig. 2. Considering HQSS, we replace the above D and D_s mesons with the D^* and D_s^* mesons, dynamically generating the D_{s1} . In the following, we introduce the effective Lagrangian approach to calculate the decay constants of molecules.

The effective Lagrangians for the $D^{(*)}(D_s^{(*)})$ mesons transitioning to the $K(\eta)$ mesons and W boson are given by


 FIG. 2. Feynman diagrams for the W boson transitioning to $D_{s0}^*(2317)$ in the DK and $D_s\eta$ molecular picture.

$$\begin{aligned}
 \mathcal{L}_{VDK} &= f_1^{DK}(0) V^\mu (D \partial_\mu K - \partial_\mu DK), & \mathcal{L}_{D_{s0}^* DK} &= g_{D_{s0}^* DK} D_{s0}^* DK, & \mathcal{L}_{D_{s0}^* D_s \eta} &= g_{D_{s0}^* D_s \eta} D_{s0}^* D_s \eta, \\
 \mathcal{L}_{VD_s \eta} &= f_1^{D_s \eta}(0) V^\mu (D_s \partial_\mu \eta - \partial_\mu D_s \eta), & \mathcal{L}_{D_{s1} D^* K} &= g_{D_{s1} D^* K} D_{s1}^\mu D_\mu^* K, & \mathcal{L}_{D_{s1} D_s^* \eta} &= g_{D_{s1} D_s^* \eta} D_{s1}^\mu D_{s\mu}^* \eta, \\
 \mathcal{L}_{AD^* K} &= (m_D + m_{K^*}) A_1^{DK^*}(0) A^\mu D_\mu^* K, & & & & \\
 \mathcal{L}_{AD_s^* \eta} &= (m_{D_s} + m_\phi) A_1^{D_s \phi}(0) A^\mu D_{s\mu}^* \eta, & & & &
 \end{aligned} \tag{12}$$

where $f_1^{DK}(0)$ [$f_1^{D_s \eta}(0)$] and $A_1^{DK^*}(0)$ [$A_1^{D_s \phi}(0)$] are the form factors at $q^2 = 0$. Such parameters can be determined by fitting the corresponding semileptonic branching fractions. In this work, we take the following values: $f_0^{DK} = 0.74$ [62,69,70], $A_1^{DK^*} = 0.78$, $A_1^{D_s \phi} = 0.77$ [71], $F_+^{DK} = 0.77$, $F_+^{D_s \eta} = 0.49$, $A_0^{DK^*} = 2.08$, and $A_0^{D_s \phi} = 2.13$ [72].

The effective Lagrangians describing the couplings of the hadronic molecules to their constituents are written as

where $g_{D_{s0}^* DK}$, $g_{D_{s0}^* D_s \eta}$, $g_{D_{s1} D^* K}$, and $g_{D_{s1} D_s^* \eta}$ are the coupling constants between D_{s0}^* (D_{s1}) and their constituents. In this work, we employ the contact-range EFT to dynamically generate D_{s0}^* and D_{s1} and further determine the couplings between the molecular states and their constituents from the residues of the corresponding poles, which are widely applied to study hadronic molecules [73–75].

With the above preparations, we can write the amplitude of Fig. 2 as

$$\begin{aligned}
 \mathcal{A}_a &= g_{D_{s0}^* DK} f_1^{DK}(0) \int \frac{d^4 q}{(2\pi)^4} \frac{1}{k_1^2 - m_1^2} \frac{1}{k_2^2 - m_2^2} (k_1^\mu - k_2^\mu) \varepsilon_\mu(V), \\
 \mathcal{A}_b &= g_{D_{s0}^* D_s \eta} f_1^{D_s \eta}(0) \int \frac{d^4 q}{(2\pi)^4} \frac{1}{k_1^2 - m_1^2} \frac{1}{k_2^2 - m_2^2} (k_1^\mu - k_2^\mu) \varepsilon_\mu(V),
 \end{aligned} \tag{14}$$

where the subscripts 1 and 2 denote the D and K mesons in amplitude \mathcal{A}_a and the D_s and η mesons in amplitude \mathcal{A}_b . Similarly, we obtain the amplitudes describing the D_{s1} created from the vacuum as

$$\begin{aligned}
 \mathcal{A}_a &= g_{D_{s1} D^* K} (m_D + m_{K^*}) A_1^{DK^*}(0) \int \frac{d^4 q}{(2\pi)^4} \varepsilon_\mu(k_0) \frac{-g^{\mu\nu} + \frac{k_1^\mu k_1^\nu}{m_1^2}}{k_1^2 - m_1^2} \frac{1}{k_2^2 - m_2^2} \varepsilon_\nu(A), \\
 \mathcal{A}_b &= g_{D_{s1} D_s^* \eta} (m_{D_s} + m_\phi) A_1^{D_s \phi}(0) \int \frac{d^4 q}{(2\pi)^4} \varepsilon_\mu(k_0) \frac{-g^{\mu\nu} + \frac{k_1^\mu k_1^\nu}{m_1^2}}{k_1^2 - m_1^2} \frac{1}{k_2^2 - m_2^2} \varepsilon_\nu(A).
 \end{aligned} \tag{15}$$

Once the amplitudes of Fig. 2 are obtained, the decay constants $f_{D_{s0}^*}$ and $f_{D_{s1}}$ can be easily extracted considering their definitions. In the following, we show how to calculate the relevant loop functions in the dimensional regularization scheme.

With the Feynman parameter approach, we obtain the following integrals:

$$\begin{aligned}
 \int \frac{d^4 k_1}{(2\pi)^4} \frac{1}{(k_1^2 - m_1^2)} &= \frac{m_1^2}{16\pi^2} \left(\ln \frac{m_1^2}{\mu^2} - 1 \right), \\
 \int \frac{d^4 k_1}{(2\pi)^4} \frac{1}{(k_1^2 - m_1^2)[(p - k_1)^2 - m_2^2]} &= \frac{1}{16\pi^2} \int_0^1 dx \ln \frac{\Delta^2}{\mu^2}, \\
 \int \frac{d^4 k}{(2\pi)^4} \frac{k^2}{(k_1^2 - m_1^2)[(p - k_1)^2 - m_2^2]} &= \frac{1}{16\pi^2} \int_0^1 dx \left[\Delta^2 \left(2 \left(\ln \frac{\Delta^2}{\mu^2} - 1 \right) + 1 \right) + p^2 x^2 \ln \frac{\Delta^2}{\mu^2} \right], \\
 \int \frac{d^4 k}{(2\pi)^4} \frac{k_1^\mu k_1^\nu}{(k_1^2 - m_1^2)[(p - k_1)^2 - m_2^2]} &= \frac{1}{16\pi^2} \int_0^1 dx \left[g^{\mu\nu} \frac{\Delta^2}{2} \left(\ln \frac{\Delta^2}{\mu^2} - 1 \right) + p^\mu p^\nu x^2 \ln \frac{\Delta^2}{\mu^2} \right],
 \end{aligned} \tag{16}$$

where $\Delta^2 = p^2x^2 - m_1^2(x-1) - x(p^2 - m_2^2)$, $p = k_1 + k_2$, and the renormalization scale μ depends on the specific physical process under consideration. To extract the decay constants of $D_{s_0}^*$ (2317) and D_{s_1} (2460), the loop functions of Eqs. (14) and (15) are converted into the following forms:

$$\int \frac{d^4k_1}{(2\pi)^4} \frac{k_1^\mu - k_2^\mu}{(k_1^2 - m_1^2)[(p - k_1)^2 - m_2^2]} = \frac{p^\mu}{16\pi^2} \int_0^1 dx (2x - 1) \ln \frac{\Delta^2}{\mu^2},$$

$$\int \frac{d^4k_1}{(2\pi)^4} \frac{-g^{\mu\nu} + \frac{k_1^\mu k_1^\nu}{m_1^2}}{(k_1^2 - m_1^2)[(p - k_1)^2 - m_2^2]} = -\frac{1}{16\pi^2} \int_0^1 dx \left\{ g^{\mu\nu} \left[\ln \frac{\Delta^2}{\mu^2} - \frac{1}{2m_1^2} \Delta^2 \left(\ln \frac{\Delta^2}{\mu^2} - 1 \right) \right] - \frac{1}{m_1^2} p^\mu p^\nu x^2 \ln \frac{\Delta^2}{\mu^2} \right\}. \quad (17)$$

Finally, we obtain the analytic form of the decay constants of $D_{s_0}^*$ (2317) and D_{s_1} (2460),

$$f_{D_{s_0}^*}^{m_1 m_2} = g_{D_{s_0}^* m_1 m_2} f_1^{m_1 m_2}(0) \frac{1}{16\pi^2} \int_0^1 dx (2x - 1) \ln \frac{\Delta^2}{\mu^2}, \quad (18)$$

$$f_{D_{s_1}}^{m_1 m_2} = \frac{g_{D_{s_1} m_1 m_2} (m_1 + m_2) A_1^{m_1 m_2}(0)}{m_{D_{s_1}}} \frac{1}{16\pi^2} \int_0^1 dx \left[\frac{1}{2m_1^2} \Delta^2 \left(\ln \frac{\Delta^2}{\mu^2} - 1 \right) - \ln \frac{\Delta^2}{\mu^2} \right], \quad (19)$$

where m_1 and m_2 refer to $D(D_s)$ and $K(\eta)$ for $D_{s_0}^*$ (2317) and $D^*(D_s^*)$ and $K(\eta)$ for D_{s_1} (2460). The decay constants of $D_{s_0}^*$ (2317) and D_{s_1} (2460) are calculated as the sum of $f_{D_{s_0}^*}^{DK}$ and $f_{D_{s_0}^*}^{D_s\eta}$ and the sum of $f_{D_{s_1}}^{D^*K}$ and $f_{D_{s_1}}^{D_s\eta}$.

C. Contact-range EFT approach

In the following, we briefly introduce the contact-range EFT approach. The scattering amplitude T is responsible for the dynamical generations of molecules and is obtained by solving the following Lippmann-Schwinger equation:

$$T(\sqrt{s}) = (1 - VG(\sqrt{s}))^{-1}V, \quad (20)$$

where V is the coupled-channel potential determined by the contact-range EFT approach and $G(\sqrt{s})$ is the loop function of the two-body propagator.

The coupled-channel potentials V in matrix form read

$$V_{DK-D_s\eta}^{J^P=0^+} = \begin{pmatrix} -2C_a & \sqrt{3}C_a \\ \sqrt{3}C_a & 0 \end{pmatrix},$$

$$V_{D^*K-D_s^*\eta}^{J^P=1^+} = \varepsilon(k_1) \cdot \varepsilon(k_1') \begin{pmatrix} -2C_a & \sqrt{3}C_a \\ \sqrt{3}C_a & 0 \end{pmatrix}, \quad (21)$$

where the coefficient C_a needs to be determined by fitting the $D_{s_0}^*$ and D_{s_1} masses. The loop functions of $D_{s_0}^*$ and D_{s_1} are

$$G(\sqrt{s})^{D_{s_0}^*} = \frac{1}{16\pi^2} \int_0^1 dx \ln \frac{\Delta^2}{\mu^2},$$

$$G(\sqrt{s})^{D_{s_1}} = \frac{1}{16\pi^2} \int_0^1 dx \left[\ln \frac{\Delta^2}{\mu^2} - \frac{1}{2m_1^2} \Delta^2 \left(\ln \frac{\Delta^2}{\mu^2} - 1 \right) \right], \quad (22)$$

with $\Delta^2 = sx^2 - m_1^2(x-1) - x(s - m_2^2)$. We note that the loop function of D_{s_1} contains an additional term, which is induced by the $\frac{k_1^\mu k_1^\nu}{m_1^2}$ term in the loop integral. One can see that the loop integrals depend on the renormalization scale μ .

With the potentials obtained above, we can search for poles generated by the coupled-channel interactions and determine the couplings between the molecular states and their constituents from the residues of the corresponding poles,

$$g_i g_j = \lim_{\sqrt{s} \rightarrow \sqrt{s_0}} (\sqrt{s} - \sqrt{s_0}) T_{ij}(\sqrt{s}), \quad (23)$$

where g_i denotes the coupling of channel i to the dynamically generated state and $\sqrt{s_0}$ is the pole position.

III. RESULTS AND DISCUSSIONS

In Table I we tabulate the masses and quantum numbers of relevant particles. One can see that there exists an unknown parameter μ (renormalization scale) in both Eqs. (17) and (22), for which a consistent value is adopted in this work. First, we employ the contact-range EFT approach to dynamically generate the poles corresponding to $D_{s_0}^*$ (2317) and D_{s_1} (2460) by varying μ and then obtain the $D_{s_0}^*$ (2317) and D_{s_1} (2460) couplings to their constituents as well as their decay constants. With the so-obtained decay constants $f_{D_{s_0}^*}$ (2317) and $f_{D_{s_1}}$ (2460), we further study the productions of $D_{s_0}^*$ (2317) and D_{s_1} (2460) in the $B_{(s)}$ and $\Lambda_b(\Xi_b)$ decays, where the naive factorization approach works well, as mentioned above. In this work, assuming that the decay mechanisms of $H_b \rightarrow H_c D_s^*$ (H_b and H_c denote bottom and charm hadrons of interest) and $H_b \rightarrow H_c D_{s_0}^*$ (D_{s_1}) are the

TABLE I. Masses and quantum numbers of relevant hadrons needed in this work [29].

Hadron	$I(J^P)$	M (MeV)	Hadron	$I(J^P)$	M (MeV)	Hadron	$I(J^P)$	M (MeV)
K^\pm	$1/2(0^-)$	493.677	K^0	$1/2(0^-)$	497.611	Λ_b	$0(1/2^+)$	5619.60
\bar{D}^0	$1/2(0^-)$	1864.84	D^-	$1/2(0^-)$	1869.66	Λ_c^+	$0(1/2^+)$	2286.46
\bar{D}^{*0}	$1/2(1^-)$	2006.85	D^{*-}	$1/2(1^-)$	2010.26	B^+	$1/2(0^-)$	5279.34
J/ψ	$0(1^-)$	3096.90	η_c	$0(0^-)$	2983.90	B^0	$1/2(0^-)$	5279.65
D_s^\pm	$0(0^-)$	1968.35	$D_s^{*\pm}$	$0(1^-)$	2112.2	B_s^0	$0(0^-)$	5366.91

TABLE II. $D_{s0}^*(2317)$ and $D_{s1}(2460)$ couplings to their constituents (in units of GeV).

Couplings	$\mu = 1.00$	$\mu = 1.50$	$\mu = 2.00$	Fu <i>et al.</i> [36]
$g_{D_{s0}^*DK}$	11.75	11.92	11.95	9.4
$g_{D_{s0}^*D_s\eta}$	8.13	7.47	7.32	7.4
$g_{D_{s1}D^*K}$	12.06	12.16	12.15	10.1
$g_{D_{s1}D_s^*\eta}$	8.78	7.76	7.53	7.9

same,¹ we parametrize the unknown nonfactorization contributions with the effective Wilson coefficients. In other words, we determine a_1 by reproducing the experimental branching fractions of $H_b \rightarrow H_c D_s^{(*)}$ decays, and then calculate the branching fractions of the corresponding decays $H_b \rightarrow H_c D_{s0}^*(D_{s1})$ using the so-obtained a_1 .

In Refs. [14,79,80] the loop function was regularized in the dimensional regularization scheme, which shows that μ is around 1.5 GeV in the charm sector. To quantify the uncertainty of the renormalization scale, we vary μ from 1 to 2 GeV in this work. For a μ of 1.0, 1.5, and 2.0 GeV, the values of C_a for $DK - D_s\eta$ ($D^*K - D_s^*\eta$) contact-range potentials are determined as 74.78, 34.53, and 25.04 (98.60, 42.45, and 30.34). With the so-obtained scattering amplitude T , we obtain the $D_{s0}^*(2317)$ and $D_{s1}(2460)$ couplings to their constituents shown in Table II, a bit different from the estimations of Ref. [36].² Finally, the decay constants of $D_{s0}^*(2317)$ and $D_{s1}(2460)$ are determined, as shown in Table III. One can see that $f_{D_{s0}^*(2317)}$ is almost independent of the renormalization scale, as can also be seen from Eq. (18). The slight variation of $f_{D_{s0}^*(2317)}$ stems from the weak dependence of the couplings $g_{D_{s0}^*DK}$

¹The productions of the $D_s^{(*)}$ mesons in the b -flavored decays mainly occur via short-distance interactions, while those of the $D_{s0}^*(D_{s1})$ mesons mainly occur via long-distance interactions due to the exotic properties of the $D_{s0}^*(D_{s1})$ mesons. The effects of long-range interactions in these decays are induced by final-state interactions via triangle diagrams [76–78]. In this work, the long-distance effects are embodied in the decay constants of $D_{s0}^*(D_{s1})$ mesons, implying that the production mechanisms of the $D_{s0}^*(D_{s1})$ mesons in b -flavored decays are similar to those of the $D_s^{(*)}$ mesons.

²One should note that an additional parameter, e.g., the subtraction constant, was introduced in Ref. [36].

and $g_{D_{s0}^*D_s\eta}$ on the renormalization scale μ . However, the decay constant $f_{D_{s1}(2460)}$ is dependent on μ , as shown in Table VI. In the following calculations, we adopt the values of $f_{D_{s0}^*(2317)}$ and $f_{D_{s1}(2460)}$ at $\mu = 1.5$ GeV, e.g., $f_{D_{s0}^*} = 58.74$ MeV and $f_{D_{s1}} = 133.76$ MeV, which are consistent with the results of Ref. [41] but smaller than the results of lattice QCD [23].

Up to now, $D_{s0}^*(2317)$ and $D_{s1}(2460)$ have only been observed in B decays. Therefore, we first focus on the decays of $B \rightarrow \bar{D}^{(*)}D_s^{(*)}$ and $B \rightarrow \bar{D}^{(*)}D_{s0}^*(D_{s1})$. In Table IV we present the parameters of the form factors in the $B \rightarrow D$ and $B \rightarrow D^*$ transitions, which are taken from Ref. [64]. By reproducing the experimental branching fractions of the decays $B \rightarrow \bar{D}^{(*)}D_s^{(*)}$, we determine the effective Wilson coefficient a_1 . Using a_1 and $f_{D_{s0}^*}(f_{D_s})$ obtained above, we calculate the branching fractions of the decays $B \rightarrow \bar{D}^{(*)}D_{s0}^*(D_{s1})$, which are shown in Table V. Our results are a bit smaller than those of Ref. [41] because of the smaller values for the decay constants and the effective Wilson coefficient. Interestingly, our results are consistent with our previous calculations using the triangle mechanism except for the decay $B^+ \rightarrow \bar{D}^{*0}D_{s0}^{*+}$ [56],³ which indicates that the triangle diagram and tree diagram accounting for the decays $B \rightarrow \bar{D}^{(*)}D_{s0}^*(D_{s1})$ are equivalent. In principle, one can replace the triangle diagram with one vertex, resulting in an effective description for the weak decay $B^+ \rightarrow \bar{D}^0D_{s0}^{*+}(2317)$ at tree level, as shown in Fig. 3, which indicates that it is reasonable to extract the decay constants of hadronic molecules using the triangle mechanism. In Ref. [55], with this approach, we extracted the decay constants of $X(3872)$ as a $\bar{D}D^*$ molecule. Here, we note that the relative phase among various amplitudes may lead to uncertainties in extracting the decay constants. As a result, it is better to select a relevant amplitude with no or small relative phases.

With the experimental branching fractions of the decays of $B^+ \rightarrow \bar{D}^0D_{s0}^{*+}(2317)$ and $B^+ \rightarrow \bar{D}^0D_{s1}^{*+}(2460)$, we

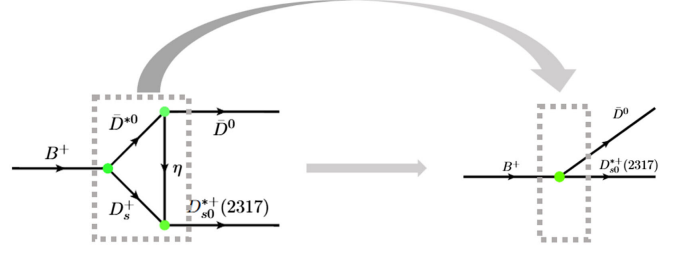
³We note that in the triangle diagram the relative phase between the $D^{(*)}$ exchange and the η exchange is fixed in such a way that they add constructively, which produces results in better agreement with data. This may not hold in the decay of $B^+ \rightarrow \bar{D}^{*0}D_{s0}^{*+}$.

TABLE III. Decay constants of D_{s0}^* (2317) and D_{s1} (2460) as hadronic molecules (in units of MeV).

Decay constants	$\mu = 1000$	$\mu = 1500$	$\mu = 2000$	Faessler <i>et al.</i> [41]
$f_{D_{s0}^*}(2317)$	59.36	58.74	58.59	67.1
$f_{D_{s1}}(2460)$	56.10	133.76	187.48	144.5

obtain the decay constants $f_{D_{s0}^*} = 75.83$ MeV and $f_{D_{s1}} = 199.75$ MeV, corresponding to physical D_{s0}^* and D_{s1} as mixtures of molecular and $c\bar{s}$ components. With the obtained $f_{D_{s0}^*}^M = 58.74$ MeV and $f_{D_{s1}}^M = 133.76$ MeV in the molecular picture as well as the proportions of the molecular components in the total wave functions, e.g., 70% and 50% [11,28], one can obtain the decay constants $f_{D_{s0}^*}^B = 115.71$ MeV and $f_{D_{s1}}^B = 265.74$ MeV, which correspond to the picture where D_{s0}^* and D_{s1} are pure excited $c\bar{s}$ states. Table VI shows the decay constants of D_{s0}^* and D_{s1} as pure $c\bar{s}$ excited states calculated by several approaches, which are consistent with our estimations and further support the picture where D_{s0}^* and D_{s1} are mainly hadronic molecules but contain sizable $c\bar{s}$ components. As a result, it is understandable that the branching fractions of the decays $B \rightarrow \bar{D}^{(*)}D_{s0}^*(D_{s1})$ in our calculations are lower than the experimental data.

Along this line, we investigate the decays of $B_s \rightarrow \bar{D}_s^{(*)}D_s^{(*)}$ and $B_s \rightarrow \bar{D}_s^{(*)}D_{s0}(D_{s1})$, which are related to the decays of $B \rightarrow \bar{D}^{(*)}D_s^{(*)}$ and $B \rightarrow \bar{D}^{(*)}D_{s0}^*(D_{s1})$ via SU(3)-flavor symmetry, as shown in Fig. 1. The amplitudes for the decays of $B_s \rightarrow \bar{D}_s^{(*)}D_s^{(*)}$ and $B_s \rightarrow \bar{D}_s^{(*)}D_{s0}(D_{s1})$ are the same as those of their SU(3)-symmetric partners.


 FIG. 3. Equivalence of the triangle diagram and the tree diagram depict the decay of $B^+ \rightarrow \bar{D}^0 D_{s0}^{*+}(2317)$.

The unknown parameters in the form factors of the $B_s \rightarrow \bar{D}_s^{(*)}D_s^{(*)}$ transitions are taken from Ref. [64] and tabulated in Table IV. Following the same strategy, we calculate the branching fractions of the decays $B_s \rightarrow \bar{D}_s^{(*)}D_{s0}^*$ and $B_s \rightarrow \bar{D}_s^{(*)}D_{s1}$. The results are shown in Table VII. One can see that the branching fractions of $D_{s0}^*(2317)$ and $D_{s1}(2460)$ in the B_s decays are similar to those in the B decays, following the SU(3)-flavor symmetry. Such large production rates mean that the $D_{s0}^*(2317)$ and $D_{s1}(2460)$ are likely to be detected in future experiments.

In addition to the productions of $D_{s0}^*(2317)$ and $D_{s1}(2460)$ in the $B_{(s)}$ decays, it is interesting to investigate their productions in the $\Lambda_b(\Xi_b)$ decays. As indicated in Fig. 1, the decays of $\Lambda_b \rightarrow D_s^{(*)}\Lambda_c$ and $\Lambda_b \rightarrow D_{s0}^*(D_{s1})\Lambda_c$ share the same mechanism as those of $B \rightarrow D_s^{(*)}\bar{D}^{(*)}$ and $B \rightarrow D_{s0}^*(D_{s1})\bar{D}^{(*)}$ at the quark level, which proceed via the decays $b \rightarrow c\bar{c}s$. In terms of SU(3)-flavor symmetry, we also investigate the decays of $\Xi_b \rightarrow D_s^{(*)}\Xi_c$ and $\Xi_b \rightarrow D_{s0}^*(D_{s1})\Xi_c$. With the naive factorization approach, the amplitudes for these decays are given by the effective Lagrangian shown in Eq. (9), where the parameters in the

 TABLE IV. Values of $F(0)^{B \rightarrow D^{(*)}}$, $a^{B \rightarrow D^{(*)}}$, $b^{B \rightarrow D^{(*)}}$ in the $B \rightarrow D^{(*)}$ transition form factors and $F(0)^{B_s \rightarrow D_s^{(*)}}$, $a^{B_s \rightarrow D_s^{(*)}}$, $b^{B_s \rightarrow D_s^{(*)}}$ in the $B_s \rightarrow D_s^{(*)}$ transition form factors [64].

	F_0	F_1	V	A_0	A_1	A_2		F_0	F_1	V	A_0	A_1	A_2
$F(0)^{B \rightarrow D^{(*)}}$	0.67	0.67	0.77	0.68	0.65	0.61	$F(0)^{B_s \rightarrow D_s^{(*)}}$	0.67	0.67	0.75	0.66	0.62	0.57
$a^{B \rightarrow D^{(*)}}$	0.63	1.22	1.25	1.21	0.60	1.12	$a^{B_s \rightarrow D_s^{(*)}}$	0.69	1.28	1.37	1.33	0.76	1.25
$b^{B \rightarrow D^{(*)}}$	-0.01	0.36	0.38	0.36	0.00	0.31	$b^{B_s \rightarrow D_s^{(*)}}$	0.07	0.52	0.67	0.63	0.13	0.56

 TABLE V. Branching fractions (10^{-3}) of $B \rightarrow \bar{D}^{(*)}D_{s0}^*(D_{s1})$.

Decay modes	Experiments [29]	a_1	Decay modes	Ours	Triangle [56]	Experiments [29]
$B^+ \rightarrow \bar{D}^0 D_s^+$	9.0 ± 0.9	0.80	$B^+ \rightarrow \bar{D}^0 D_{s0}^{*+}(2317)$	0.48	0.68	$0.80_{-0.13}^{+0.16}$
$B^+ \rightarrow \bar{D}^{*0} D_s^+$	8.2 ± 1.7	0.93	$B^+ \rightarrow \bar{D}^{*0} D_{s0}^{*+}(2317)$	0.39	1.21	$0.90_{-0.70}^{+0.70}$
$B^+ \rightarrow \bar{D}^0 D_s^{*+}$	7.6 ± 1.6	0.81	$B^+ \rightarrow \bar{D}^0 D_{s1}^+(2460)$	1.39	1.26	$3.1_{-0.9}^{+1.0}$
$B^+ \rightarrow \bar{D}^{*0} D_s^{*+}$	17.1 ± 2.4	0.83	$B^+ \rightarrow \bar{D}^{*0} D_{s1}^{*+}(2460)$	4.36	3.07	12.0 ± 3.0

TABLE VI. Decay constants of $D_{s0}^*(2317)$ and $D_{s1}(2460)$ as the excited states (in units of MeV).

Decay constants	$f_{D_{s0}^*}$	$f_{D_{s1}}$
QCD sum rule [81]	333 ± 20	345 ± 17
Quark model [43]	110	233
Salpeter method [82]	112	219
Covariant light-front quark model [64]	$74.4_{-10.6}^{+10.4}$	159_{-32}^{+36}
Lattice QCD [23]	$114(2)(0)(+5)(10)$	$194(3)(4)(+5)(10)$
Ours	115.71	265.74

form factors of the $\Lambda_b \rightarrow \Lambda_c$ and $\Xi_b \rightarrow \Xi_c$ transitions are obtained in the quark model [65,66,83] and tabulated in Table VIII. The decay constants of the charmed-strange mesons $D_s^{(*)}$ and $D_{s0}^*(D_{s1})$ are calculated in the same way as explained above.

One should note that only the branching fraction of the decay $\Lambda_b \rightarrow D_s \Lambda_c$ is available in the RPP. Very recently, the ratio of $\mathcal{B}(\Lambda_b \rightarrow D_s^* \Lambda_c) / \mathcal{B}(\Lambda_b \rightarrow D_s \Lambda_c) = 1.688 \pm 0.022_{-0.055}^{+0.061}$ was reported by the LHCb Collaboration [84] and one can obtain the branching fraction of the decay $\Lambda_b \rightarrow D_s^* \Lambda_c$. With the branching fractions of $\mathcal{B}(\Lambda_b \rightarrow D_s \Lambda_c)$ and $\mathcal{B}(\Lambda_b \rightarrow D_s^* \Lambda_c)$ as inputs, we determine a_1 and then predict the branching fractions of the decays of $\Lambda_b \rightarrow D_{s0}^* \Lambda_c$ and $\Lambda_b \rightarrow D_{s1} \Lambda_c$, which are shown in Table IX. We can see that the production rates of $D_{s0}^*(2317)$ and $D_{s1}(2460)$ in the Λ_b decay are of the order of 10^{-3} , which are large enough to be detected in future experiments. Since the effective Wilson coefficients in the B decays and B_s decays are similar, as shown in Tables V and VII, we can take the same values for a_1 in the Λ_b decays and the Ξ_b decays. Similarly, we predict the branching fractions of the decays $\Xi_b \rightarrow D_s^{(*)} \Xi_c$ and $\Xi_b \rightarrow D_{s0}^*(D_{s1}) \Xi_c$ in Table IX. The production rates of ground-state mesons $D_s^{(*)}$ and excited mesons $D_{s0}^*(D_{s1})$ in the Ξ_b decays are of the order of 10^{-2} and 10^{-3} , which are likely to be detected in future experiments. In Ref. [48], the authors estimated the ratios $\mathcal{B}(\Lambda_b \rightarrow \Lambda_c M) / \mathcal{B}(B \rightarrow DM)$, where M represents the ground-state $D_s^{(*)}$ and excited $D_{s0}^*(D_{s1})$ mesons. In Table X we show the ratios $R_u^M = \mathcal{B}(\Lambda_b \rightarrow \Lambda_c M) / \mathcal{B}(B \rightarrow DM)$ and $R_s^M = \mathcal{B}(\Xi_b \rightarrow \Xi_c M) / \mathcal{B}(B_s \rightarrow D_s M)$ obtained in this work, which are consistent with

 TABLE VIII. Values of $F(0)$, a , b in the $\Lambda_b \rightarrow \Lambda_c$ and $\Xi_b \rightarrow \Xi_c$ transition form factors [65,66].

	F_1^V	F_2^V	F_3^V	F_1^A	F_2^A	F_3^A
$F(0)^{\Lambda_b \rightarrow \Lambda_c}$	0.549	0.110	-0.023	0.542	0.018	-0.123
$a^{\Lambda_b \rightarrow \Lambda_c}$	1.459	1.680	1.181	1.443	0.921	1.714
$b^{\Lambda_b \rightarrow \Lambda_c}$	0.571	0.794	0.276	0.559	0.255	0.828
$F(0)^{\Xi_b \rightarrow \Xi_c}$	0.467	0.145	0.086	0.447	-0.035	-0.278
$a^{\Xi_b \rightarrow \Xi_c}$	1.702	2.530	1.742	1.759	2.675	2.270
$b^{\Xi_b \rightarrow \Xi_c}$	0.531	1.581	0.758	0.356	1.789	1.072

 TABLE IX. Branching fractions (10^{-3}) of $\Lambda_b \rightarrow \Lambda_c D_{s0}^*(D_{s1})$ and $\Xi_b \rightarrow \Xi_c D_{s0}^*(D_{s1})$.

Decay modes	Experiments		Decay modes	Ours
	[29,84]	a_1		
$\Lambda_b \rightarrow \Lambda_c D_s$	11 ± 1.0	0.88	$\Lambda_b \rightarrow \Lambda_c D_{s0}^*(2317)$	0.70
$\Lambda_b \rightarrow \Lambda_c D_s^*$	18.568 ± 1.102	0.76	$\Lambda_b \rightarrow \Lambda_c D_{s1}(2460)$	4.34
Decay modes	Ours	a_1	Decay modes	Ours
$\Xi_b \rightarrow \Xi_c D_s$	8.52	0.88	$\Xi_b \rightarrow \Xi_c D_{s0}^*(2317)$	0.58
$\Xi_b \rightarrow \Xi_c D_s^*$	16.30	0.76	$\Xi_b \rightarrow \Xi_c D_{s1}(2460)$	4.29

 TABLE X. Ratios of $R_u^M = \mathcal{B}(\Lambda_b \rightarrow \Lambda_c M) / \mathcal{B}(B \rightarrow DM)$ and $R_s^M = \mathcal{B}(\Xi_b \rightarrow \Xi_c M) / \mathcal{B}(B_s \rightarrow D_s M)$.

R_u^M	Ours	Reference [48]	R_s^M	Ours
$R_u^{D_s}$	1.22	1.75	$R_s^{D_s}$	1.94
$R_u^{D_s^*}$	2.44	3.47	$R_s^{D_s^*}$	2.35
$R_u^{D_{s0}^*}$	1.46	1.58	$R_s^{D_{s0}^*}$	1.23
$R_u^{D_{s1}}$	3.12	4.76	$R_s^{D_{s1}}$	3.64

Ref. [48]. We can see that the production rates of ground-state mesons $D_s^{(*)}$ and excited mesons $D_{s0}^*(D_{s1})$ in the $\Lambda_b(\Xi_b)$ decays are larger than those in the $B(B_s)$ decays because the $\Lambda_b \rightarrow \Lambda_c(\Xi_b \rightarrow \Xi_c)$ form factors are larger than the corresponding $B(B_s) \rightarrow D(B_s)$ form factors, as shown in Ref. [48].

IV. SUMMARY AND OUTLOOK

In this work, we utilized the effective Lagrangian approach to compute the decay constants of $D_{s0}^*(2317)$

 TABLE VII. Branching fractions (10^{-3}) of $B_s \rightarrow \bar{D}_s^{(*)} D_{s0}^*(D_{s1})$.

Decay modes	Experiments [29]	a_1	Decay modes	Ours
$B_s^0 \rightarrow D_s^+ D_s^-$	4.4 ± 0.5	0.87	$B_s^0 \rightarrow D_s^- D_{s0}^{*+}(2317)$	0.47
$B_s^0 \rightarrow D_s^{*+} D_s^- + D_s^+ D_s^{*-}$	13.9 ± 1.7	0.83	$B_s^0 \rightarrow D_s^{*-} D_{s0}^{*+}(2317)$	0.27
$B_s^0 \rightarrow D_s^{*+} D_s^- + D_s^+ D_s^{*-}$	13.9 ± 1.7	0.77	$B_s^0 \rightarrow D_s^- D_{s1}^+(2460)$	1.18
$B_s^0 \rightarrow D_s^{*+} D_s^-$	14.4 ± 2.1	0.84	$B_s^0 \rightarrow D_s^{*-} D_{s1}^+(2460)$	4.11

and $D_{s1}(2460)$ as hadronic molecules dynamically generated by the $DK - D_s\eta$ and $D^*K - D_s^*\eta$ contact-range potentials, and then with the naive factorization approach systematically investigated the productions of $D_{s0}^*(2317)$ and $D_{s1}(2460)$ in the $B_{(s)}$ and $\Lambda_b(\Xi_b)$ decays, which proceed via the decay $b \rightarrow c\bar{c}s$ at the quark level. The decay constants of $D_{s0}^*(2317)$ and $D_{s1}(2460)$ are estimated to be 58.74 MeV and 133.76 MeV. In particular, the decay constant of $D_{s0}^*(2317)$ is almost independent of the renormalization scale μ in the loop functions.

As for the branching fractions of the decays $B \rightarrow \bar{D}^{(*)}D_{s0}^*(2317)$ and $B \rightarrow \bar{D}^{(*)}D_{s1}(2460)$, our results are smaller than the experimental data but are consistent with our previous results obtained in the triangle mechanism, which indicates that $D_{s0}^*(2317)$ and $D_{s1}(2460)$ may contain components other than hadronic molecules such as the $c\bar{s}$ cores. The values of $\mathcal{B}[B_s \rightarrow \bar{D}_s^{(*)}D_{s0}^*(2317)]$ and $\mathcal{B}[B_s \rightarrow \bar{D}_s^{(*)}D_{s1}(2460)]$ are similar to those of $\mathcal{B}[B \rightarrow \bar{D}^{(*)}D_{s0}^*(2317)]$ and $\mathcal{B}[B \rightarrow \bar{D}^{(*)}D_{s1}(2460)]$, which reflect the underlying SU(3)-flavor symmetry. In addition, we predicted the branching fractions of the decays $\Lambda_b \rightarrow \Lambda_c D_{s0}^*(2317)$ and $\Lambda_b \rightarrow \Lambda_c D_{s1}(2460)$ as well as $\Xi_b \rightarrow \Xi_c D_{s0}^*(2317)$ and $\Xi_b \rightarrow \Xi_c D_{s1}(2460)$, which are much larger than the corresponding ones in the B and B_s decays and indicate that the productions of $D_{s0}^*(2317)$ and

$D_{s1}(2460)$ in the decays of bottom baryons are likely to be detected in future experiments.

Our study shows that, because of the equivalence of the triangle mechanism to the tree diagram established in calculating the branching fractions of the decays $B \rightarrow \bar{D}^{(*)}D_{s0}^*(2317)$ and $B \rightarrow \bar{D}^{(*)}D_{s1}(2460)$, one can extract the decay constants of $D_{s0}^*(2317)$ and $D_{s1}(2460)$ as hadronic molecules via the triangle mechanism. This provides an effective approach for calculating the decay constants of hadronic molecules, which can then be used in studies of these hadronic molecules in other related processes. We hope that our present work can stimulate more studies along this line.

ACKNOWLEDGMENTS

We are grateful to Professor Fu-Sheng Yu for stimulating discussions. This work is supported in part by the National Natural Science Foundation of China under Grants No. 11975041 and No. 11961141004. M.-Z. L acknowledges support from the National Natural Science Foundation of China under Grant No. 12105007. X.-Z. L acknowledges support from the National Natural Science Foundation of China under Grant No. 12247159 and the China Postdoctoral Science Foundation under Grant No. 2022M723149.

-
- [1] B. Aubert *et al.* (BABAR Collaboration), *Phys. Rev. Lett.* **90**, 242001 (2003).
- [2] D. Besson *et al.* (CLEO Collaboration), *Phys. Rev. D* **68**, 032002 (2003); **75**, 119908(E) (2007).
- [3] Y. Mikami *et al.* (Belle Collaboration), *Phys. Rev. Lett.* **92**, 012002 (2004).
- [4] M. Ablikim *et al.* (BESIII Collaboration), *Phys. Rev. D* **97**, 051103 (2018).
- [5] P. Krokovny *et al.* (Belle Collaboration), *Phys. Rev. Lett.* **91**, 262002 (2003).
- [6] B. Aubert *et al.* (BABAR Collaboration), *Phys. Rev. Lett.* **93**, 181801 (2004).
- [7] B. Aubert *et al.* (BABAR Collaboration), *Phys. Rev. D* **69**, 031101 (2004).
- [8] S. Godfrey and N. Isgur, *Phys. Rev. D* **32**, 189 (1985).
- [9] Q.-T. Song, D.-Y. Chen, X. Liu, and T. Matsuki, *Phys. Rev. D* **91**, 054031 (2015).
- [10] M. Albaladejo, P. Fernandez-Soler, J. Nieves, and P. G. Ortega, *Eur. Phys. J. C* **78**, 722 (2018).
- [11] Z. Yang, G.-J. Wang, J.-J. Wu, M. Oka, and S.-L. Zhu, *Phys. Rev. Lett.* **128**, 112001 (2022).
- [12] S.-Q. Luo, B. Chen, X. Liu, and T. Matsuki, *Phys. Rev. D* **103**, 074027 (2021).
- [13] T. Barnes, F. E. Close, and H. J. Lipkin, *Phys. Rev. D* **68**, 054006 (2003).
- [14] D. Gamermann, E. Oset, D. Strottman, and M. J. Vicente Vacas, *Phys. Rev. D* **76**, 074016 (2007).
- [15] F.-K. Guo, P.-N. Shen, H.-C. Chiang, R.-G. Ping, and B.-S. Zou, *Phys. Lett. B* **641**, 278 (2006).
- [16] Z.-X. Xie, G.-Q. Feng, and X.-H. Guo, *Phys. Rev. D* **81**, 036014 (2010).
- [17] M. Cleven, F.-K. Guo, C. Hanhart, and U.-G. Meissner, *Eur. Phys. J. A* **47**, 19 (2011).
- [18] Z.-H. Guo, U.-G. Meißner, and D.-L. Yao, *Phys. Rev. D* **92**, 094008 (2015).
- [19] T.-W. Wu, M.-Z. Liu, L.-S. Geng, E. Hiyama, and M. P. Valderrama, *Phys. Rev. D* **100**, 034029 (2019).
- [20] L. Liu, K. Orginos, F.-K. Guo, C. Hanhart, and U.-G. Meissner, *Phys. Rev. D* **87**, 014508 (2013).
- [21] D. Mohler, C. B. Lang, L. Leskovec, S. Prelovsek, and R. M. Woloshyn, *Phys. Rev. Lett.* **111**, 222001 (2013).
- [22] C. B. Lang, L. Leskovec, D. Mohler, S. Prelovsek, and R. M. Woloshyn, *Phys. Rev. D* **90**, 034510 (2014).
- [23] G. S. Bali, S. Collins, A. Cox, and A. Schäfer, *Phys. Rev. D* **96**, 074501 (2017).
- [24] C. Alexandrou, J. Berlin, J. Finkenrath, T. Leontiou, and M. Wagner, *Phys. Rev. D* **101**, 034502 (2020).
- [25] S. Weinberg, *Phys. Rev.* **137**, B672 (1965).
- [26] A. Martínez Torres, E. Oset, S. Prelovsek, and A. Ramos, *J. High Energy Phys.* **05** (2015) 153.

- [27] M. Albaladejo, D. Jido, J. Nieves, and E. Oset, *Eur. Phys. J. C* **76**, 300 (2016).
- [28] J. Song, L. R. Dai, and E. Oset, *Eur. Phys. J. A* **58**, 133 (2022).
- [29] R. L. Workman *et al.* (Particle Data Group), *Prog. Theor. Exp. Phys.* **2022**, 083C01 (2022).
- [30] Fayyazuddin and Riazuddin, *Phys. Rev. D* **69**, 114008 (2004).
- [31] S. Ishida, M. Ishida, T. Komada, T. Maeda, M. Oda, K. Yamada, and I. Yamauchi, *AIP Conf. Proc.* **717**, 716 (2004).
- [32] W. Wei, P.-Z. Huang, and S.-L. Zhu, *Phys. Rev. D* **73**, 034004 (2006).
- [33] M. Nielsen, *Phys. Lett. B* **634**, 35 (2006).
- [34] A. Faessler, T. Gutsche, V. E. Lyubovitskij, and Y.-L. Ma, *Phys. Rev. D* **76**, 014005 (2007).
- [35] A. Faessler, T. Gutsche, V. E. Lyubovitskij, and Y.-L. Ma, *Phys. Rev. D* **76**, 114008 (2007).
- [36] H.-L. Fu, H. W. Griesshammer, F.-K. Guo, C. Hanhart, and U.-G. Meißner, *Eur. Phys. J. A* **58**, 70 (2022).
- [37] Y. Huang, M.-Z. Liu, Y.-W. Pan, L.-S. Geng, A. Martínez Torres, and K. P. Khemchandani, *Phys. Rev. D* **101**, 014022 (2020).
- [38] T.-W. Wu, Y.-W. Pan, M.-Z. Liu, and L.-S. Geng, *Sci. Bull.* **67**, 1735 (2022).
- [39] T.-C. Wu and L.-S. Geng, *Phys. Rev. D* **108**, 014015 (2023).
- [40] B. Aubert *et al.* (BABAR Collaboration), *Phys. Rev. D* **74**, 032007 (2006).
- [41] A. Faessler, T. Gutsche, S. Kovalenko, and V. E. Lyubovitskij, *Phys. Rev. D* **76**, 014003 (2007).
- [42] P. Colangelo, G. Nardulli, A. A. Ovchinnikov, and N. Paver, *Phys. Lett. B* **269**, 201 (1991).
- [43] S. Veseli and I. Dunietz, *Phys. Rev. D* **54**, 6803 (1996).
- [44] H.-Y. Cheng, C.-K. Chua, and C.-W. Hwang, *Phys. Rev. D* **69**, 074025 (2004).
- [45] P. Colangelo, F. De Fazio, and A. Ozpineci, *Phys. Rev. D* **72**, 074004 (2005).
- [46] H.-Y. Cheng and C.-K. Chua, *Phys. Rev. D* **74**, 034020 (2006).
- [47] J. Segovia, C. Albertus, E. Hernandez, F. Fernandez, and D. R. Entem, *Phys. Rev. D* **86**, 014010 (2012).
- [48] A. Datta, H. J. Lipkin, and P. J. O'Donnell, *Phys. Rev. D* **69**, 094002 (2004).
- [49] Z.-W. Liu, J.-X. Lu, and L.-S. Geng, *Phys. Rev. D* **107**, 074019 (2023).
- [50] N. Ikeno, G. Toledo, and E. Oset, *Phys. Lett. B* **847**, 138281 (2023).
- [51] STAR Collaboration, *Nature (London)* **527**, 345 (2015).
- [52] ALICE Collaboration, *Nature (London)* **588**, 232 (2020); **590**, E13 (2021).
- [53] L.-L. Chau, *Phys. Rep.* **95**, 1 (1983).
- [54] L.-L. Chau and H.-Y. Cheng, *Phys. Rev. D* **36**, 137 (1987); **39**, 2788(A) (1989).
- [55] Q. Wu, M.-Z. Liu, and L.-S. Geng, *Eur. Phys. J. C* **84**, 147 (2024).
- [56] M.-Z. Liu, X.-Z. Ling, L.-S. Geng, En-Wang, and J.-J. Xie, *Phys. Rev. D* **106**, 114011 (2022).
- [57] A. Ali, G. Kramer, and C.-D. Lu, *Phys. Rev. D* **58**, 094009 (1998).
- [58] A. Ali, G. Kramer, Y. Li, C.-D. Lu, Y.-L. Shen, W. Wang, and Y.-M. Wang, *Phys. Rev. D* **76**, 074018 (2007).
- [59] H.-n. Li, C.-D. Lu, and F.-S. Yu, *Phys. Rev. D* **86**, 036012 (2012).
- [60] M. Bauer, B. Stech, and M. Wirbel, *Z. Phys. C* **34**, 103 (1987).
- [61] H.-Y. Cheng and B. Tseng, *Phys. Rev. D* **48**, 4188 (1993).
- [62] H.-Y. Cheng and C.-W. Chiang, *Phys. Rev. D* **81**, 074021 (2010).
- [63] T. Gutsche, M. A. Ivanov, J. G. Körner, and V. E. Lyubovitskij, *Phys. Rev. D* **98**, 074011 (2018).
- [64] R. C. Verma, *J. Phys. G* **39**, 025005 (2012).
- [65] T. Gutsche, M. A. Ivanov, J. G. Körner, V. E. Lyubovitskij, P. Santorelli, and N. Habył, *Phys. Rev. D* **91**, 074001 (2015); **91**, 119907(E) (2015).
- [66] R. N. Faustov and V. O. Galkin, *Phys. Rev. D* **98**, 093006 (2018).
- [67] H.-Y. Cheng, *Phys. Rev. D* **56**, 2799 (1997); **99**, 079901(E) (2019).
- [68] C. E. Thomas, *Phys. Rev. D* **73**, 054016 (2006).
- [69] H.-Y. Cheng, C.-W. Chiang, and A.-L. Kuo, *Phys. Rev. D* **93**, 114010 (2016).
- [70] J. Zhang, C.-X. Yue, and C.-H. Li, *Eur. Phys. J. C* **78**, 695 (2018).
- [71] Q. Chang, X.-N. Li, and L.-T. Wang, *Eur. Phys. J. C* **79**, 422 (2019).
- [72] M. A. Ivanov, J. G. Körner, J. N. Pandya, P. Santorelli, N. R. Soni, and C.-T. Tran, *Front. Phys. (Beijing)* **14**, 64401 (2019).
- [73] C. W. Xiao, J. Nieves, and E. Oset, *Phys. Rev. D* **100**, 014021 (2019).
- [74] M.-L. Du, V. Baru, F.-K. Guo, C. Hanhart, U.-G. Meißner, J. A. Oller, and Q. Wang, *Phys. Rev. Lett.* **124**, 072001 (2020).
- [75] Y.-W. Pan, M.-Z. Liu, and L.-S. Geng, *Phys. Rev. D* **108**, 114022 (2023).
- [76] H.-Y. Cheng, C.-K. Chua, and A. Soni, *Phys. Rev. D* **71**, 014030 (2005).
- [77] F.-S. Yu, H.-Y. Jiang, R.-H. Li, C.-D. Lü, W. Wang, and Z.-X. Zhao, *Chin. Phys. C* **42**, 051001 (2018).
- [78] Y. Cao, Y. Cheng, and Q. Zhao, *arXiv:2303.00535*.
- [79] R. Molina, T. Branz, and E. Oset, *Phys. Rev. D* **82**, 014010 (2010).
- [80] C. Chen, C. Meng, Z.-G. Xiao, and H.-Q. Zheng, *arXiv:2307.12069*.
- [81] Z.-G. Wang, *Eur. Phys. J. C* **75**, 427 (2015).
- [82] G.-L. Wang, *Phys. Lett. B* **650**, 15 (2007).
- [83] J.-X. Lu, M.-Z. Liu, R.-X. Shi, and L.-S. Geng, *Phys. Rev. D* **104**, 034022 (2021).
- [84] R. Aaij *et al.* (LHCb Collaboration), *arXiv:2311.14088*.